

# Fabrication and Properties of a Hybrid Biocompatible Nanofiber Mesh Constituted of Polycaprolactone and Self-Assembly Peptide

Yang Yang<sup>1,\*</sup>, Bingyin Shuai<sup>2</sup>

<sup>1</sup>Zhejiang Yunmao Technology Co., Ltd., Hangzhou, China

<sup>2</sup>Zhejiang Runfeng Energy Group Co., Ltd., Hangzhou, China

## Email address:

yang.yang1@xyb2b.com (Yang Yang), shuaiby@zju.edu.cn (Bingyin Shuai)

\*Corresponding author

## To cite this article:

Yang Yang, Bingyin Shuai. Fabrication and Properties of a Hybrid Biocompatible Nanofiber Mesh Constituted of Polycaprolactone and Self-Assembly Peptide. *Advances in Materials*. Vol. 12, No. 1, 2023, pp. 1-8. doi: 10.11648/j.am.20231201.11

**Received:** December 4, 2022; **Accepted:** December 27, 2022; **Published:** January 10, 2023

---

**Abstract:** Conventional therapeutic methods for organ and tissue deficiencies include surgical reconstruction, organ transplantation, medical devices treatment, synthetic prosthesis and so on, of which the application is limited when donors exhibit a low availability and impaired organs and tissues cannot well perform their functions. Tissue Engineering (TE) can harmonize with regional organs or tissues, ensure optimal degradation time for novel structure rebirth, facilitate cell adhesiveness, contribute to cell procreation and differentiation in tissue scaffolds, etc., making it an alternative option for treating pathological obstacles. Artificial polymers such as polycaprolactone (PCL) and nature materials such as peptides are adopted for the fabrication of nanofiber scaffolds. The study first engineered porous PCL scaffolds for examining the fiber morphology and the diameter alternations considering the change of single variable condition of the solution concentration, voltage and electrode distance, etc., thereby finding the basic conditions for producing nanofiber scaffolds with good formation. With the increase in solution concentration, the more obvious molecule entanglement can limit the jet stretching, thereby enlarging the fiber diameters. Voltage negatively impacts the fiber diameters, and elevated voltage can strengthen the electric intensity, thereby leading to a complete stretching of cone jets and making fiber diameters thinner. Besides, increased electrode distance is followed by expanded flight distance and decreased electrode intensity (constant voltage), as a result, fibers become narrower. Nanofiber substance exhibits the optimal performance under the condition of solution concentration: 6%, voltage: 50kV, and electrode distance: 150mm. Subsequently, nanofiber scaffolds were fabricated based on the respective preparation of PCL/P11-4 and PCL/P11-8 polymer solutions. Both P11-4 and P11-8 presented uneven distribution in PCL scaffolds, which involved various PCL nanofiber substances with abundant peptides. PCL nanofiber scaffolds saw the breakage of P11-4 and P11-8 fibers.

**Keywords:** Tissue Engineering, Polycaprolactone, Peptides, Nanofiber Scaffolds

---

## 1. Introduction

Tissue and organ grafting, as a common treatment method for pathological problem and inadequate body tissue or organs, is limited by the availability of donors. Also, surgical reconstruction, medical device, synthetic prostheses, etc., fail to be well applied due to the limited function of impaired tissues or organs [1]. Tissue Engineering (TE) is a clinical application technique integrating engineering technology and biological technology, aiming to compensate the deficient tissue and organ functions and substitute traditional

therapeutic method. In the reconstruction process of tissues or organs, there are basically two categories of TE.

- 1) cell-free engineered scaffolds can serve as temporary scaffolds in injured tissue defects, together with the regeneration of injured tissues in vivo.
- 2) cell-incorporated engineered scaffolds can cause the regeneration of injured tissues in vitro, which contribute to substrates for cell adhesion, proliferation and differentiation. Novel tissues are formed during the degradation of scaffolds.

We selected synthetic polymers (polycaprolactone,

polydioxanones, poly (lactic acid), poly (lac-tic-co-glycolic acid), poly (ethylene-co-vinyl acetate), and PU, etc.) together with natural materials (peptides, chitosan, collagen, and gelatin, etc.) for the production of nanofiber scaffolds. TE scaffolds share similar characteristics as natural ECM, thereby playing their functions in the healing process, assisting in the reconstruction of novel body tissues in human bodies. Our Study are focusing on producing nanofibers by changing solution concentration, applied voltages, electrodes distances via NanoSpider and achieve the followings:

- 1) Found out optimal conditions to produce well formed nanofibers;
- 2) Decrease fiber diameters to the range of 400-800nm;
- 3) Testing properties of the well formed nanofibers.

### 1.1. Peptide Material Advantages and Disadvantages

Self-assembly peptide materials are characterized by biodegradability, biocompatibility, simple structure, relatively stable mechanical and chemical properties, diverse molecular architecture and arrangement, and large-scale manufacturing practicability, hence enjoying an extensive application in the files of TE, antimicrobial agent, and drug delivery mediated by carriers, etc. [2] However, their mechanical strengths are not sufficient to support cells as that can be done by human tissues [3].

Peptides can be self-assembled from disordered molecules to organized structure experiencing from monomer, tape, ribbon, fibril, to fiber phases [4]. This self-assembly process is affected by its intrinsic properties like peptide sequence, amount of amino acids, and attractive interactions within peptides e.g. hydrogen bonding, electrostatic forces, hydrophobic, Wan de Waals interactions as well as surrounding circumstances including pH, temperature, additives of salts, varied constitutions of the solution and solution aging time [5]. Existing the critical concentration, below which, peptide self-assembly property would improve with the increasing amount of the peptide; whereas, when peptide is above the critical concentration, there is no big difference by adding peptides [6].

P11-8, P11-12 and P11-14 which containing +2, +2, and +4 net charges separately display critical concentrations for self-assembly ( $C^*$ ) of P11-8, P11-12 and P11-14 around 440uM, 2300uM and >10,000uM individually. Additionally, P11-14 self-assembly process is restricted due to the high electrostatic repulsive force of +4 net charge compared with other peptides [7]. As a result, higher critical concentration of self-assembly ( $C^*$ ) of this peptide is obtained. Moreover, the equilibrium within solutions can be obtained much quicker while concentration is lower than critical concentration for self-assembly ( $C^*$ ).

There exists one of the dominant parameters-pH during the reversible and autonomous process. Peptide phase transition from fluid to gel or the other way around can be simply induced by changing solution pH. Taking P11-4, P11-5 and P11-8 as an example, at low pH=2, P11-4 forms fibrils. However, P11-4 phase changes from fibrils to monomer fluid phase by increasing pH. At the pH range from 6.8 to 7.2, gel

to fluid transition happens. Nevertheless, P11-4 is pH dependent. When P11-4 concentration is lower than 10mg/ml, peptides can be dissolved in the solution at the pH around 7, and assemble to gel at the pH of 1-4.2; but it can also form hydrogel at the pH 7.4 with the concentration higher than 10mg/ml as well as the additives of 140mM salts [8].

In contrast, P11-5 and P11-8 can only form gel at high pH, and P11-8 experiences fluid, fluid-gel coexisting and gel phases. Therefore, peptide self-assembly process can be simply promoted or prevented by adding acids or base.

Crossing linking in the peptide gel can be promoted by increasing ionic strength-by adding salts within solution which induces the attractions between neighboring fibrils e.g. hydrogen bonding and hydrophobic forces. Furthermore, ions in the salts can form salt bridge between peptides, e.g. adding NaCl to the solution of P11-4 at high pH, Glu--Na+-Glu- salt bridges are formed with the presence of Na<sup>+</sup>, leading to the formation of peptide gel at high pH. In Figure 2, by adding 130mM NaCl to 10mg/mL to the P11-4 solution, transition from  $\beta$ -sheet to monomer state increases 4 pH unites. However, 130mM NaCl in the 10mg/mL P11-8 lowers the process from  $\beta$ -sheet to monomer state for 3 pH unites [9].

Interaction forces within the self-assembled peptide nanofiber or gel can be conquered by the extraneous energy e.g. increased temperature which means transition from self-assembled peptide gel to monomer phase can be induced by increasing the ambient temperature. During the self-assembly process, different peptide phases can be observed along the aging time. For example, anti-parallel  $\beta$ -sheets are formed progressively based on the formation of  $\beta$  sheets [8].

### 1.2. Polycaprolactone (PCL) Advantages and Disadvantages

Polycaprolactone (PCL) refers to a biodegradable polymer of which the melting point is 60°C and the glass transition temperature is -60°C, and it has been approved to be applied in human body by FDA. Specifically, TE scaffolds adopt PCL for the rehabilitation of tissue defects and membranes for guiding the regeneration of bones. PCL can also be applied in the dentistry industry for the night guards (dental splints) and root canal filling. The fabrication process is relied on the ring-opening polymerization (ROP) of  $\epsilon$ -caprolactone under the catalysis of dibutyl zinc triisobutyl aluminum such as stannous octoate [10]. PCL fabrication process is as follows.

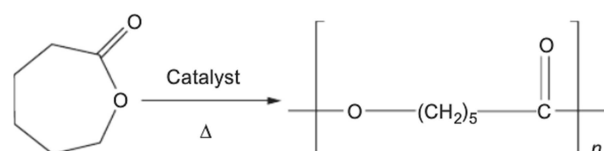


Figure 1. Synthesis of Polycaprolactone (Kumbar et al., 2014).

Determining mechanical properties for optimum nanofibre scaffolds include suitably particular fibril strength and elasticity of the nanofibres, but most importantly, proper

polymer degradation time. Degradation properties are affected by polymer type. In general, synthetic fibers like PCL, PLA and others have longer degradation time than natural fibers. As a semicrystalline aliphatic polyester, PCL has a degradation time around 2 to 4 years, whereas, it varies when mixed with other biodegradable polymers [11]. And the degradation process is associated by hydrolysis of its ester linkage in physiological conditions, therefore, it has been widely utilized as the implantable biomaterial [12]. Apart from the fiber type, nanofibers with smaller fiber diameters degrade faster than those with larger ones. Whereas, degradation property of scaffolds should be engineered based on the tissue type. For example, scaffolds for bone tissue should be rigid enough to sustain cells, accordingly, scaffolds are designed with polymers of low degradation rate and bigger diameter sizes. In contrast, skin scaffolds are typically engineered to be mixed with natural polymers, e.g., collagen with small diameter size to obtain the ultimate tissue elasticity and deformability [13]. PCL features strong physical strength, and is biodegradable and biocompatible, hence enjoying a broad application in tissue engineering and drug delivery, etc. [14] Despite this, PCL also exhibits surface hydrophobicity, and the secondary structure of the absorbed proteins on the surface changes, which impacts the blood biocompatibility. Hence, the surface hydrophobicity and hydrophilicity shall be balanced.

### **1.3. Advantages of PCL and Self-Assembly Peptide Scaffolds**

Self-assembly peptides can enhance the hydrophilicity exhibited by PCL scaffolds, as stem cells can not adhere to circumstances with strong hydrophobicity or strong hydrophilicity. Hence, scaffolds integrating PCL and self-assembly peptides strengthen stem cell adhesion, proliferation, and differentiation within the scaffolds on the one hand, and mechanically support stem cells on the other hand [15, 16].

### **1.4. Nanofiber Scaffolds**

Pores within tissue engineering scaffolds are comparable to most bio-molecules in size. Therefore, these molecules e.g. drugs, proteins, nucleic acid therapeutics and others can not only be circulated but also act as the components within the scaffolds [17]. And structure of nanofiber scaffolds e.g. porosity of the membrane is highly depending on the fiber diameter [18].

Construction and physical properties of the tissue scaffolds can be affected by hydrophobicity of the polymers. Higher hydrophobicity of the polymers will lead to better mechanical strength of the scaffolds. Moreover, it would be easier for the formation of the scaffolds [19]. Niknam et al. [20] also point out it would be easier for cells to adhere and diffuse on the hydrophilic rather than hydrophobic exterior. Nanofibers serve as tissue engineering scaffolds exhibit optimal dominance due to the high surface area-to-volume ratio. Moreover, its architecture is similar to extracellular

matrix (ECM).

### **1.5. Needleless Electrospinning**

Electrospinning technology has been widely utilized to yield nano-scale fibers for the applications of tissue engineering, wound dressing, drug delivery, filtration etc. since 1934 when it was firstly introduced. However, traditional needle-based electrospinning technology meets the vital deficiencies, e.g., low production rate of 0.3g/m and only single jet can be formed from needle generator. Consequently, productivity is improved by increasing feed-rate and concentration or by applying “multi-needle electrospinning”. Whereas, disadvantages of these methods might be raised fiber diameters as well as intensive labor work and unsatisfactory fiber morphology respectively [21].

Needleless electrospinning technology was introduced in 1979 and commercialized in 2005 by Elmarco. According to Qin et al. [22], jets are formed from open solution surface which is driven by electric field intensity. During this process, surface tension is conquered by the repulsive electrostatic force, jets are drawn towards the collector associated with evaporation of solvents, subsequently, nanofibers with diameters ranging from 50nm to 1000nm are accumulated on the collector.

Needleless electrospun nanofiber scaffold expresses superior properties like high surface-to-volume ratio; hugely porous structures with admirable pore conjunctions; diameters within nano-scale; primary physical properties; controllable in fiber diameter, morphology and resulted web architecture etc. [23]

Needleless electrospinning process can be greatly affected by the vital elements to control resulted fiber diameter, morphology, web density, porosity and so on. The influencing parameters includes concentration, viscosity, conductivity and surface tension of the applied solution; varied conditions of the device e.g. voltage, distance between electrodes, electrode rotational rate and electric field intensity as well as the temperature, relative humidity and air flow rate of the surrounding conditions.

### **1.6. Spinnability of the Solution and Its Affecting Parameters**

Spinnability of the solution is determinant aspect during the electrospinning process. Since it may lead to the spray or beads formation in the resulted nanofibers with low spinnability of the solutions. Generally speaking, solution spinnability largely depends on its viscoelasticity and capacity to be electrospun continuously without fiber breakage [24]. In short, affecting parameters of the solution spinnability can be concluded as followed.

According to A dictionary of chemical engineering, viscosity is construed to measure dynamic performance of the solution. It can be defined that a specific liquid would bear the shear resistance between neighboring solution layers due to the molecular tension within the solution. It is used to explain that some liquids like gas, water etc. can move easily

while others like treacle or glycerine cannot. Viscosity of a particular liquid can be determined by its the characteristics of polymers and solvents.

In general, viscoelastic force of formed jets during electrospinning process can be increased due to the raised viscosity of the solution, which in turn prevents further change of the flying jets. Accordingly, it leads to higher diameters of resulted nanofibers [25]. Makhmudovna [26] points out that viscosity of the solution mainly depends on molecular weight of polymer, polymer concentration within solution and solvent properties.

Dielectric constant  $\epsilon$  of the solution signifies the capacity of the solution to reserve electrical energy. Electrospinning technology favors solvents with higher dielectric constant. Since electrical energy reserved in the solution increased with the dielectric constant, and solution containing higher electric storage requires longer time for the depletion of the energy. As a result, jets are better stretched by electric force, leading to the thinner fiber diameters and higher porosity of the scaffolds. PCL nanofibers can be electrospun when the dielectric constant is higher than 19 at the temperature of 20°C. In short, electrospinnability of the solution via Nanospider can be improved by increasing dielectric constant of the solution which is expressed as the less and smaller bead formation on the resulted mats [27].

Solubility of a polymer in specific solvent is a prior aspect of spinnability of the solution via NanoSpider. Polymers with higher solubility can easily interface with their solvents. Since these polymer can magnify the molecular interplay between them and solvents. Whereas, polymers with lower solubility encourage polymer-polymer connection, leading to the separation of the polymer within solution [28].

## 2. Materials and Methods

### 2.1. Materials and Solution Preparation

Poly ( $\epsilon$ -caprolactone) (PCL) (Mn80,000) and 1,1,1,3,3,3-Hexafluoro-2-propanol (HFIP) were provided by Sigma-Aldrich, used for fabricating different concentrations of PCL nanofiber webs (6%, 5% and 4%). P11-4 (94.9%) and P11-8 (77.8%) came from C S Bio Co. PCL was dissolved in the HFIP solvent (6% (w/w)) to prepare PCL/P11-4 mixture (2.5ml) and PCL/P11-8 mixture (2.5ml), respectively. 50mg P11-4 or 50mg P11-8 were then be added into each of them. Solutions were maintained for one night to ensure the homogeneity.

### 2.2. Needleless Electrospinning- Nanospider<sup>TM</sup> Technology

The NanoSpider<sup>TM</sup> NS200 (Elmarco) was employed for obtaining nanofibers from PCL or PCL/peptides mixture. Figure 2 illustrates the fabrication process of nanofibers by it. NanoSpider<sup>TM</sup> NS200 is composed by a rotating electrode (a) which acts as a positive roller in polymer solution (c) and a metal collector (b) for obtaining the textile substitute (d). Fiber webs which have various diameters and fiber morphologies

can be obtained by controlling the solution concentration, voltage and electrode distance.

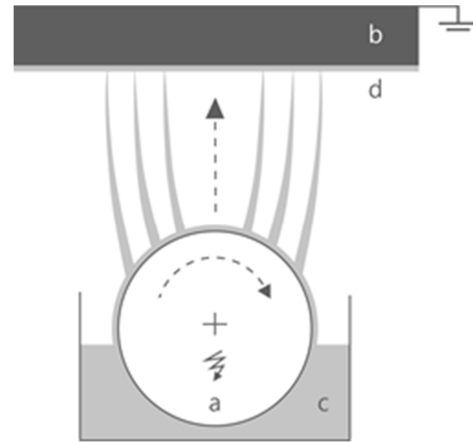


**Figure 2.** The apparatus of Nanospider<sup>TM</sup> technology includes a rotating electrode (a) acting as a positive roller, a collector (b) for obtaining textile substitute (d), and polymer solution (c).

### 2.3. Scanning Electron Microscope - Fiber Morphology Analysis

Scanning electron microscope (SEM) served for analyzing the fiber morphology, and during the process, Quorum Q150RS was employed. We placed resulted nanofiber webs on small metal plates and coated them with a thin gold layer. The apparatus mark Joe model JSM-5310 served for the examination of the specimens.

### 2.4. Image Analysis Computer-Fiber Diameter Measurement

Image analysis computer is utilized to analysis the fiber diameters based on the fiber images attained from SEM. Nanofiber webs were prepared to get average diameter of each sample. At least 150 fiber diameters of each nanofiber samples were measured to get the average diameter of each fiber substitute.

## 3. Results and Discussion

### 3.1. Polycaprolactone (PCL) Fiber Morphology Analysis

Before the statistical analysis on the variation of fiber diameter, we obtained the general fiber morphology of different PCL fibers from SEM images. These fibers were obtained under the conditions of solution concentration: 6%, voltage: 50kV, and electrode distance: 150mm. Figure 3 (a) displays the high-magnification images of fibers which have different fiber diameters and morphologies. Figure 3 (b) shows the variation of fiber diameters in the range of 397.37nm-13000nm, and such variation can be obviously affected by the solution concentration, voltage and electrode distance, which can be explained subsequently. Figure 3 (c) demonstrates high-spinning fibers of which the surface is rough. Figure 3 (d) shows the fibers with both rough and smooth surfaces. In the same sample, different fibers presented

different surface roughness and fiber spin, hence, the two parameters cannot be affected by the fabrication condition.

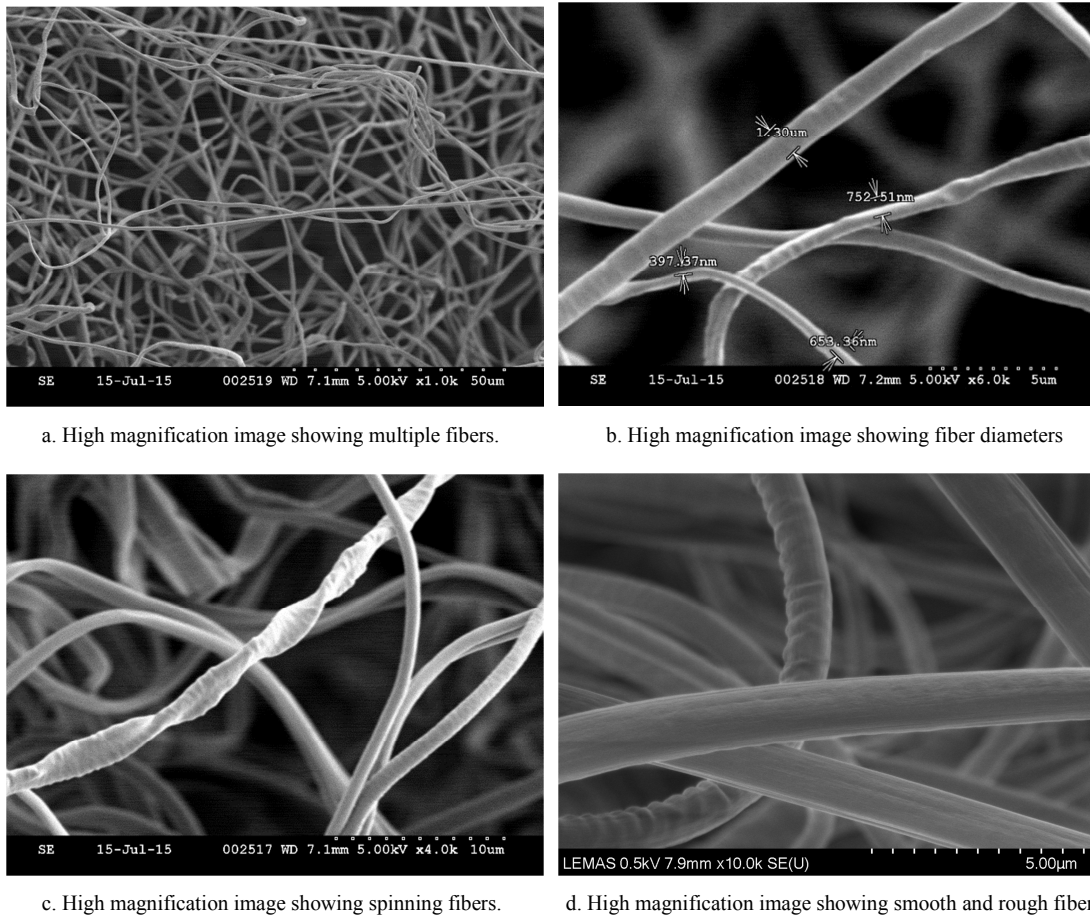
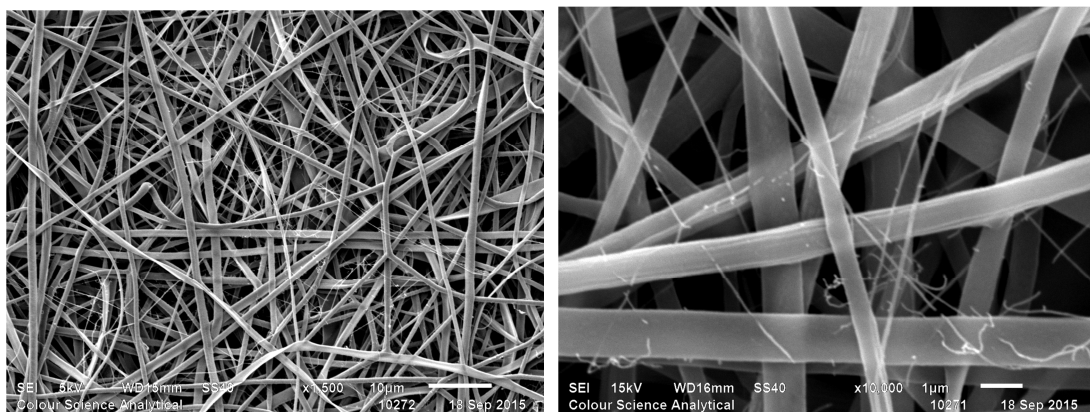


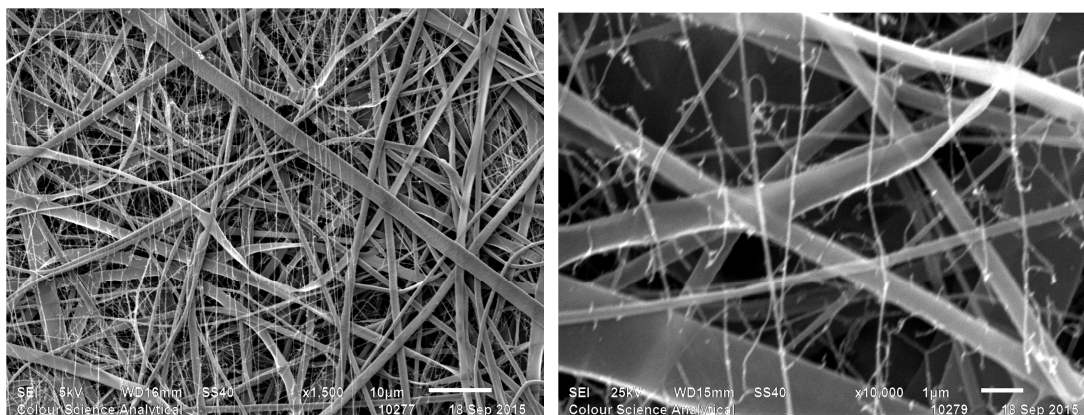
**Figure 3.** SEM images at increasing magnifications of PCL fibers samples by needleless electro-spun technology show different morphological patterns. Fibers are fabricated in the condition that solution concentration is 6%, voltage is 50kV, and electrode distance is 150mm.

### 3.2. Polycaprolactone and Self-Assembly Peptide Fiber Morphology Analysis

Figure 4 displays the SEM images about PCL/P11-4 and PCL/P11-8 fiber samples which have various fiber morphologies. Their fabrication process was conducted under the conditions of solution concentration: 6%, voltage: 50kV, and electrode distance: 150mm. Figure 4 (a) and (b) show PCL

fibers with abundant P11-4. Figure 4 (c) and (d) demonstrate the PCL/ P11-8 fiber images. Figure 4 (a) and (c) present the uneven distribution of P11-4 and P11-8 in PCL fiber scaffolds and peptides-enriched PCL fibers showed deformation and emerged to each other. Figure 4 (b) and (d) present the breakage of P11-4 and P11-8 within PCL fiber scaffolds. Based on these images, the morphology of PCL/P11-4 and PCL/P11-8 fiber showed no obvious difference.





c. Low magnification image showing PCL and P11-8 fiber multiple fibers

d. High magnification image showing PCL and P11-4 fibers

**Figure 4.** SEM images at increasing magnifications of PCL and peptide fibers samples by needleless electrospun technology show different morphological patterns. Fibers are fabricated in the condition that solution concentration is 6%, voltage is 50kV, and electrode distance is 150mm.

### 3.3. Fiber Diameter Analysis

The independent variables examined in this study are expected to influence fiber diameters. In particular, polymer solution concentration has a positive relation with viscosity, macromolecule entanglement of the solution and resulted in fiber diameters. When concentration is high, macromolecule entanglement increases which restricting bending and stretching properties of the jets, leading to smaller sedimentation area and thicker fiber diameters. When concentration (viscosity) is low, non-spinning solution is obtained and beads or mixture of beads and fibers are foamed. Figure 5 shows that average fiber diameters vary from 404nm, 358nm, to 904nm when voltage is 50kV, electrode distance is 130mm and solution concentration (w/w) change from 3%, 5%, 6%.

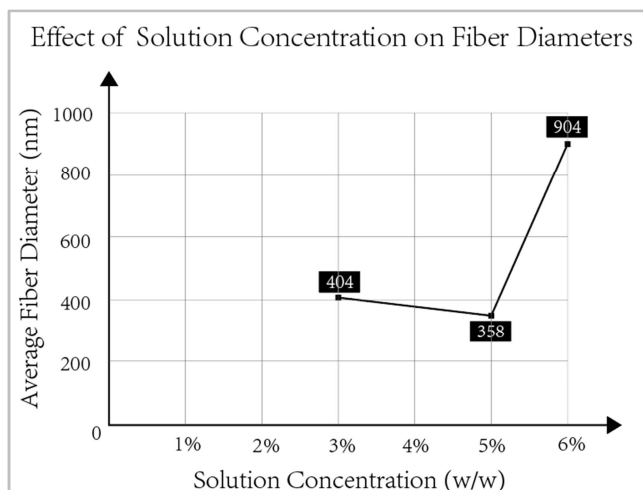


**Figure 5.** Average fiber diameters obtained when voltage is 50kV, electrode distance is 130mm and solution concentrations (w/w) change from 3%, 5% to 6%.

Voltage can only induce Taylor cone above critical voltage which depends on solution characteristics, spinneret generators and others. When voltage is high, electric fields

intensity increases accordingly. And this leads to completely stretched jets and resulting in thinner fiber diameters. In this study, fiber diameters decreased from 1540nm, 900nm, to 580nm when solution concentration (w/w) is 6%, electric distance is 130mm, and voltage changes from 40kV, 50kV to 60kV which is showed in Figure 6.

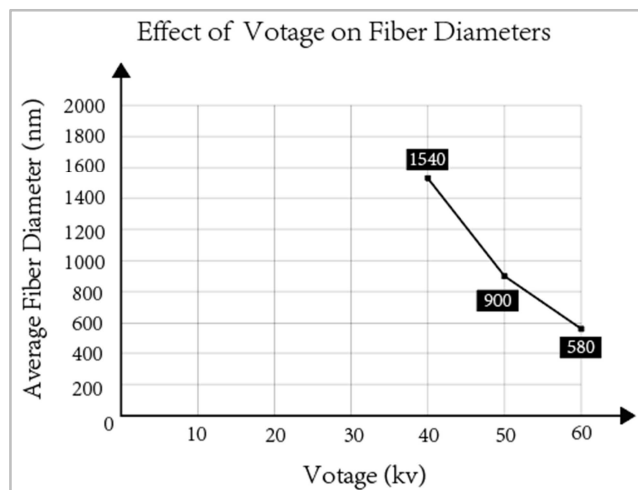


**Figure 6.** Average fiber diameters obtained when electrode distance is 130mm, solution concentrations (w/w) is 6%, and voltages (kV) change from 40kV to 60kV.

When electrode distance is high, jet flight distance increases and electric field intensity decreases (constant voltage). There existing minimal electric distance which allows complete evaporation to collect solid fibers, depending on solution properties and spinneret geometry. When electrode distance is too high, corona discharge may be caused. Generally, increased electrode distance leads to decreased fiber diameters. Figure 7 shows that average fiber diameters change from 1190nm, 900nm, 1010nm, to 760nm when voltage is 50kV, solution concentration is 6%(w/w) and electrode distance vary from 110mm, 130mm, 150mm, to 170mm.

Other affecting parameters include evaporation rate of

solvents, electric field intensity, solvent property, flight distance, solution flow rate, ambient temperature, humidity, air velocity and so on. Resulted fibers without completely evaporation leads to the moist, kinky and entangled morphology. Electric field intensity is a function of applied voltage and electrodes distance which acts as the driving force in the needleless electrospinning. Slightly increasing electric field intensity, production rate increases significantly, no big influence in the aspects of fiber diameter and fiber diameter distribution.

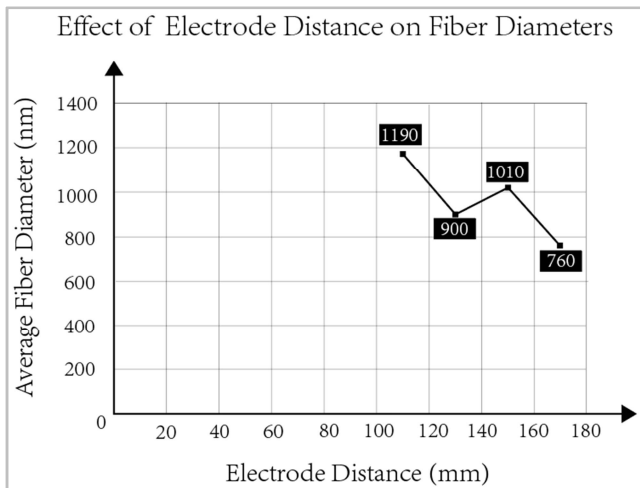


**Figure 7.** Average fiber diameters obtained when voltage is 50kV, solution concentration is 6%(w/w) and electrode distances change from 110mm to 170mm.

## 4. Conclusion

We successfully electro-spun PCL webs in the study, however, PCL/peptides nanofibers underwent deformation. In SEM images, PCL nanofibers showed various fiber morphologies, with different fiber roughness and fiber spin in the same sample, showing the irrelevance of fiber morphology to the spinning condition. In PCL/peptides substances, peptide fibers showed irregular distribution in PCL fibers and some underwent fracture within the scaffolds. Peptides-contained PCL underwent contortion. In terms of factors determining fiber diameter, solution concentration is positively related to fiber diameter because concentration increase leads to macromolecule entanglement increase, which restricts stretching properties of the jets, leading to thicker fiber diameters. Besides, the increase in voltage enhances the electric intensity, thereby leading to a thorough jet stretching and thinner fibers. Also, the elevation in electrode distance is followed by an increase in jet flight distance, thus raising the electrode distance.

The future aims of this paper are to produce well-formed nanofiber scaffolds consisting of PCL with self-assembly peptides with stages of: testing characterization of PCL/peptides nanofiber scaffolds like water contact angle measurement, tensile stress measurement and so on; cell culture in vitro test, to find out cell adhesion, proliferation and differentiation properties.

## References

- [1] Singh A P, Biswas A, Shukla A, et al. Targeted therapy in chronic diseases using nanomaterial-based drug delivery vehicles [J]. *Signal transduction and targeted therapy*, 2019, 4 (1): 1-21.
- [2] Delfi M, Sartorius R, Ashrafizadeh M, et al. Self-assembled peptide and protein nanostructures for anti-cancer therapy: Targeted delivery, stimuli-responsive devices and immunotherapy [J]. *Nano Today*, 2021, 38: 101119.
- [3] Wang Y, Zhang W, Gong C, et al. Recent advances in the fabrication, functionalization, and bioapplications of peptide hydrogels [J]. *Soft Matter*, 2020, 16 (44): 10029-10045.
- [4] Gatto E, Toniolo C, Venanzi M. Peptide Self-Assembled Nanostructures: From Models to Therapeutic Peptides [J]. *Nanomaterials*, 2022, 12 (3): 466.
- [5] Zozulia O, Korendovych I V. Semi-Rationally Designed Short Peptides Self-Assemble and Bind Hemin to Promote Cyclopropanation [J]. *Angewandte Chemie*, 2020, 132 (21): 8185-8189.
- [6] Alharbi N, Skwarczynski M, Toth I. The influence of component structural arrangement on peptide vaccine immunogenicity [J]. *Biotechnology Advances*, 2022: 108029.
- [7] Koch F, Müller M, König F, et al. Mechanical characteristics of beta sheet-forming peptide hydrogels are dependent on peptide sequence, concentration and buffer composition [J]. *Royal Society open science*, 2018, 5 (3): 171562.
- [8] Ghosh G, Barman R, Mukherjee A, et al. Control over Multiple Nano-and Secondary Structures in Peptide Self-Assembly [J]. *Angewandte Chemie International Edition*, 2022, 61 (5): e202113403.
- [9] Gascoigne L, Magana J R, Atkins D L, et al. Fractal-like R5 assembly promote the condensation of silicic acid into silica particles [J]. *Journal of Colloid and Interface Science*, 2021, 598: 206-212.
- [10] Levato R, Jungst T, Scheuring R G, et al. From shape to function: the next step in bioprinting [J]. *Advanced Materials*, 2020, 32 (12): 1906423.
- [11] Dias J R, Sousa A, Augusto A, et al. Electrospun polycaprolactone (PCL) degradation: an in vitro and in vivo study [J]. *Polymers*, 2022, 14 (16): 3397.
- [12] Barber V, Borden M, Alty J, et al. Modifying Poly (caprolactone) Degradation through C-H Functionalization [J]. 2022.
- [13] Bartnikowski M, Dargaville T R, Ivanovski S, et al. Degradation mechanisms of polycaprolactone in the context of chemistry, geometry and environment [J]. *Progress in Polymer Science*, 2019, 96: 1-20.
- [14] Atıcı B, Ünlü C H, Yanilmaz M. A review on centrifugally spun fibers and their applications [J]. *Polymer Reviews*, 2022, 62 (1): 1-64.
- [15] Nune M, Subramanian A, Krishnan U M, et al. Peptide nanostructures on nanofibers for peripheral nerve regeneration [J]. *Journal of tissue engineering and regenerative medicine*, 2019, 13 (6): 1059-1070.

- [16] Gelain F, Luo Z, Zhang S. Self-assembling peptide EAK16 and RADA16 nanofiber scaffold hydrogel [J]. *Chemical reviews*, 2020, 120 (24): 13434-13460.
- [17] Xia P, Luo Y. Vascularization in tissue engineering: The architecture cues of pores in scaffolds [J]. *Journal of Biomedical Materials Research Part B: Applied Biomaterials*, 2022, 110 (5): 1206-1214.
- [18] Jadbabaei S, Kolahdoozan M, Naeimi F, et al. Preparation and characterization of sodium alginate–PVA polymeric scaffolds by electrospinning method for skin tissue engineering applications [J]. *RSC advances*, 2021, 11 (49): 30674-30688.
- [19] Nareswari T L, Juniatic M, Aminatun A, et al. A facile technique for overcoming seeding barriers of hydrophobic polycaprolactone/hydroxyapatite-based nanofibers for bone tissue engineering [J]. *Journal of Applied Pharmaceutical Science*, 2022 (Notice: Undefined offset: 3 in/home/japsonli/public\_html/abstract.php on line 193).
- [20] Niknam Z, Golchin A, Rezaei–Tavirani M, et al. Osteogenic differentiation potential of adipose-derived mesenchymal stem cells cultured on magnesium oxide/polycaprolactone nanofibrous scaffolds for improving bone tissue reconstruction [J]. *Advanced Pharmaceutical Bulletin*, 2022, 12 (1): 142.
- [21] Moon S, Lee K J. 9 Needleless and syringeless electrospinning for mass production [J]. *Green Electrospinning*, 2019: 217.
- [22] Qin Z, Yan G, Zhang X, et al. Finite element method assisted design of needleless electrospinning systems for mass production of polymer nanofibers [J]. *Chemical Engineering Science*, 2022, 259: 117817.
- [23] Xu X, Si Y, Zhao Y, et al. Electrospun Textile Strategies in Tendon to Bone Junction Reconstruction [J]. *Advanced Fiber Materials*, 2022: 1-27.
- [24] Silva P M, Torres-Giner S, Vicente A A, et al. Management of operational parameters and novel spinneret configurations for the electrohydrodynamic processing of functional polymers [J]. *Macromolecular Materials and Engineering*, 2022: 2100858.
- [25] Gulzar S, Tagrida M, Nilsuwan K, et al. Electrospinning of gelatin/chitosan nanofibers incorporated with tannic acid and chitooligosaccharides on polylactic acid film: Characteristics and bioactivities [J]. *Food Hydrocolloids*, 2022, 133: 107916.
- [26] Makhmudovna K Z. Investigation of the Influence of the Nature of the Solvent on the Properties of Solutions of Grafted Triacetate Copolymers [J]. *Texas Journal of Multidisciplinary Studies*, 2022, 6: 86-89.
- [27] Luo C J, Stride E, Edirisinghe M. Mapping the influence of solubility and dielectric constant on electrospinning polycaprolactone solutions [J]. *Macromolecules*, 2012, 45 (11): 4669-4680.
- [28] Sivan M, Madheswaran D, Hauzerova S, et al. AC electrospinning: impact of high voltage and solvent on the electrospinnability and productivity of polycaprolactone electrospun nanofibrous scaffolds [J]. *Materials Today Chemistry*, 2022, 26: 101025.